바이오시스템공학 (*J. of Biosystems Eng.*)
Vol. 31, No. 6, pp. 489~499 (2006)

오버헤드 가이던스 레일 추종 방식에 의한 과수방제기의 무인 주행

신범수 김상헌 박재언

Autonomous-guided orchard sprayer using overhead guidance rail

B. S. Shin S. H. Kim J. U. Park

Abstract

Since the application of chemicals in confined spaces under the canopy of an orchard is hazardous work, it is needed to develop an autonomous guidance system for an orchard sprayer. The autonomous guidance system developed in this research could steer the vehicle by tracking an overhead guidance rail, which was installed on an existing frame structure. The autonomous guidance system consisted of an 80196 kc microprocessor, an inclinometer, two interface circuits of actuators for steering and ground speed control, and a fuzzy control algorithm. In addition, overhead guidance rails for both straight and curved paths were devised, and a trolley was designed to move smoothly along the overhead guidance rails. Evaluation tests showed that the experimental vehicle could travel along the desired path at a ground speed of 30 ~ 50 cm/s with a RMS error of 5 cm and maximum deviation of less than 12 cm. Even when the vehicle started with an initial offset or a deflected heading angle, it could move quickly to track the desired path after traveling 2 ~ 3 m. The vehicle could also complete turns with a curvature of 1 m. However, at a ground speed of 50 cm/s, the vehicle tended to over-steer, resulting in a zigzag motion along the straight path, and tended to turn outward from the projected line of the guidance rail.

Keywords : Autonomous guidance system, Overhead guidance rail, Orchard vehicle, Offset measurement system, Steering control

1. INTRODUCTION

Recently some farmers have grown pears in greenhouse-like frame structures to protect heavily fruited branches from being broken by windy weather. These U-shaped frames are placed upside down between two trees along the tree rows. The branches of each tree are tied up on the frame to form a Y-shape, which results in a long tunnel between the rows of trees as shown in Fig. 1. Agri-chemicals are more hazardous to orchard sprayer operators when they are working in such confined environments, closely exposed to the chemicals. Protective gear or cabs have been used to protect operators from contact with agri-chemicals. Spraying, nonetheless, is a dangerous job. An autonomous guidance technology would greatly increase safety by removing operators from spray vehicles (Cho and Ki, 1999).

Considerable efforts have been made to achieve autonomous operation of orchard sprayers. Jang et al. (1995) developed an inductive cable guidance system for guiding orchard sprayers along a buried cable. Torri (2000) reported that a driverless sprayer could follow a guidance cable buried in the ground at about 0.3 m depth with an offset error of

This work was financially supported by Agricultural R&D Promotion Center (ARPC). The article was submitted for publication in November 2006. reviewed and approved for publication by the editorial board of KSAM in December 2006. The authors are Beom Soo Shin, Professor, KSAM member, Sang Hun Kim, Professor, KSAM member, and Jae Un Park, Former Graduate Research Assistant, Dept. of Biological Systems Engineering, Kangwon National University, Chuncheon, Korea. Corresponding author: B. S. Shin, Professor, Dept. of Biological Systems Engineering, Kangwon National University, Chuncheon, 200-701, Korea; Fax: +82-33-255-6406; E-mail: <bshin@kangwon.ac.kr>.

Fig. 1 View of typical pear orchards.

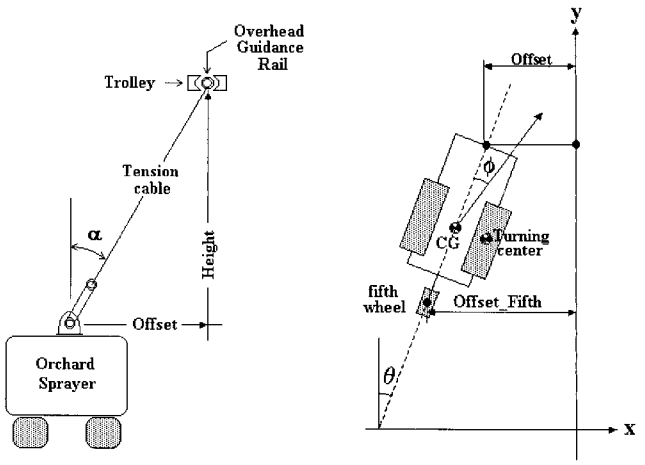

(a) viewed from rear (b) viewed from top

Fig. 2 Schematic diagram of measuring lateral offset (α: inclinometer angle, θ : heading angle of vehicle, and ϕ : steering angle).

0.1 m or less at a ground speed of 0.76 m/sec. Kim et al. (1999) developed a mechanical steering control system for a tiny battery-operated sprayer for greenhouse use. Two sets of guide rollers mounted beneath the sprayer on the front and rear forced the sprayer to move on a fixed path. However, the buried cable or auxiliary guidance pipe on the ground could be an obstacle to the feasibility of this system, due to inconvenience and limitations thereof. Shin et al. (2001) used two ultrasonic sensors for an orchard sprayer to determine its travel path by measuring the locations of targets ahead such as tree trunks or structures. This system showed the feasibility of a low-cost guidance system, but its applicability was limited due to the need to prepare the working environment to eliminate irregular reflections from leaves and/or branches. A research group used machine vision and acoustic sensors to determine the travel path by detecting the space between trees and the distance to the tree trunk (Cho and Ki, 1999). A camera had to be located at a certain height in front of the vehicle for receiving clear images of the path, to avoid interference with the low profile canopy. Various algorithms were adopted in this procedure to determine the desired paths; however, these methods experienced some difficulties when the vehicle turned at the end of a row. A DGPS was also used to monitor the position of a guidance system (Cho and Lee, 2000), increasing the reliability during the end-turn. Those developments were relatively successful; however, machine vision or GPS were not yet economically feasible and might be useless in a confined space. On the other hand, Simens and Coates (2000) tested a mobile truss of a cable-drawn farming system moving along an aboveground guidance cable. The control strategy was to maintain the front and the rear of the mobile truss at a certain distance from the guidance cable, a mechanical sensory system being adopted. Test results showed that the position errors of the mobile truss were 12 cm and 24 cm at the 99.7% and 99.9% confidence levels, respectively.

Therefore, a mechanical sensory system could be a cost-effective and reliable alternative for autonomous guidance control in orchard applications. This paper reports the development and operation of such an overhead-guidance-rail-based orchard sprayer guidance system. The lateral offset of the sprayer could be obtained from the angle made by a tension cable, connected to a point on the sprayer, with the overhead guidance rail (Fig. 2). The steering control would be made in the direction to reduce the lateral offset.

The specific objectives of this research were : 1) to modify a commercial sprayer to be an autonomously operated unit, 2) to develop an offset measurement system with an overhead guidance device, 3) to develop a steering control algorithm, and 4) to evaluate system performance through computer simulation and laboratory trials.

2. MATERIALS AND METHODS

A. Experimental vehicle with guidance control system

The experimental vehicle used in the project was a small-scale orchard sprayer (SS180-CT, Hanseo Co., Korea), 1985 x 720 x 1030 mm (length x width x height), with

crawler treads. Steering of the unmodified sprayer was executed by pulling left and right levers connected by cables to crawler clutches, working in two stages. Driving power to the crawler would be disengaged at the first stage and braked at the second stage, so that the clutches could be used for a quick skid-turn with a minimum radius (Shin et al., 2001). Figure 3 illustrates a block diagram of the proposed guidance system. It consists of an inclinometer for lateral offset measurement, two interface circuits for the two power cylinders, a controller for HST and an angular velocity sensor (rotary encoder, Autonics, Korea) for ground speed measurement. These were interfaced with an 80196kc microprocessor (Intel, U.S.A.) using its special functions such as A/D conversion, high speed input (HSI), PWM output.

This sprayer was modified to incorporate the autonomous guidance system. Two clutch- activating cables were replaced by two power cylinders (Tsubakimoto Chain Co., Japan), electrically operated by a 12 V DC power supply. The power cylinder had a maximum stroke of 50 mm with a thrust of 50 N, and was equipped with an internal protection circuit to stop excessive current flow at both ends of the stroke. The interface circuit of the power cylinder with the microprocessor was designed as shown in Fig. 4 (Shin et al., 2001). The low level signal from the microprocessor activates the relay to maintain the retracted position. When the position is at the initial stage, the electrical power to the power cylinder is cut by the internal protection circuit. When the output signal substantially rises, the piston moves forward to disengage the steering clutch at a speed of 50 mm/s. At the end of the stroke, the protection circuit is activated by an adjustable location limit switch according to the operating range of the steering clutch lever. Since it takes at least 360 ms to disengage the clutch completely, the high level signal should be maintained for a while. The same amount of time is required for re-engagement. The steering angle is, therefore, determined by the time for which the clutch remains disengaged.

In this study, the original mechanical transmission was fixed in 3rd gear and a hydrostatic transmission (HST) was inserted into the power train to provide motion controllability for the vehicle. A step motor was used to control the angular position of the hydraulic pump swash plate and a proximity sensor monitored the angle of the swash plate (Shin et al., 2001). A special marker was attached to the fifth wheel to indicate the trajectory of the vehicle on the ground surface as the vehicle traveled.

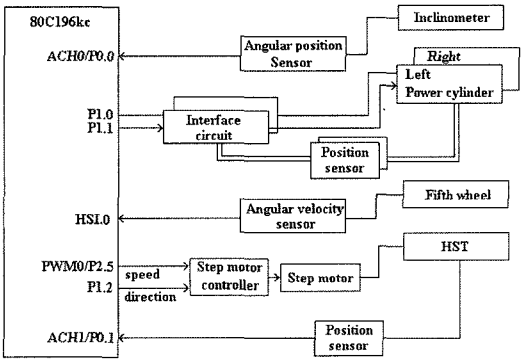

Fig. 3 Block diagram of autonomous guidance system.

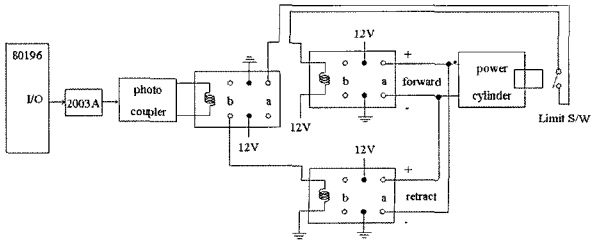

Fig. 4 Control circuit of power cylinder.

B. Offset measurement system : Inclinometer

An inclinometer was developed to measure the lateral offset of the vehicle. As shown in Fig. 5, it consists of a shaft of 0.5 m in length supported on two bearings, a rotary potentiometer attached to one end of the shaft and a tension cable. The tension cable length can be adjusted using a soft coil spring. When the vehicle moved laterally away from

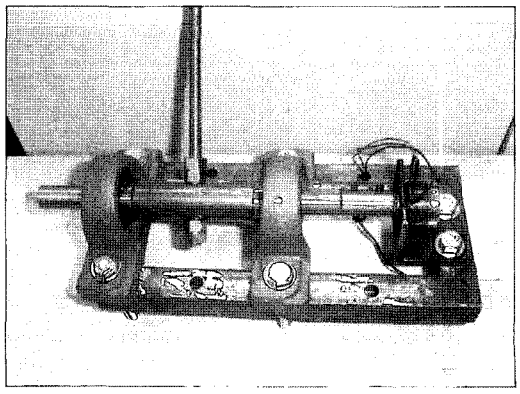

Fig. 5 View of developed inclinometer.

the projected line of the overhead guidance rail, the shaft of the inclinometer was rotated in accordance with the angle made by the tension cable, as shown in Fig. 2. The output signal from the potentiometer was directly fed into the I/O pin of the microprocessor. The inclinometer was calibrated in the range of 0° to 180° with 5 increments, resulting in Eq.(1) with R^2 of 0.9995:

$$V = 0.8983\alpha - 5.5799 \quad (1)$$

where α is the angular displacement of the inclinometer in degrees and V is the A/D converted value of the output voltage. The offset could be obtained based on the angular displacement of the inclinometer as follows :

$$Offset = \tan(\alpha) * Height \quad (2)$$

where *Height* is the vertical distance from the overhead guidance rail to the inclinometer.

C. Overhead guidance device

The overhead guidance device consists of the overhead guidance rail and trolley. A light-weight pipe (ϕ = 25 mm) was used as an overhead guidance rail. For the turns of the guidance rail, two pieces of pipe bent with a radius of 1 m were connected to make a quarter of circle. If the distance between two adjacent rows was greater than 2 m, a straight piece of pipe could be added as necessary. In this project, the distance between tree rows was set to 3 m.

A trolley was devised to roll smoothly and evenly without slip on a curved path as well as on a straight path. Also, it had to be able to swing left and right with the tension cable leads. It was made of four plastic roller bearings and a support frame as shown in Fig. 6.

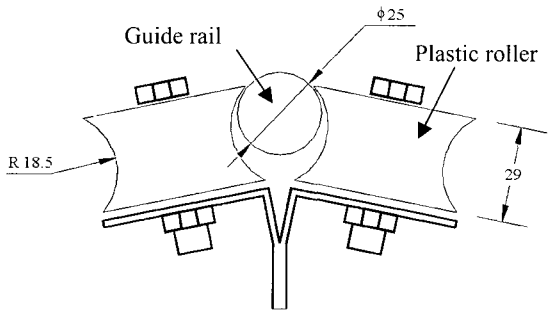

Fig. 6 Schematic diagram of trolley.

D. Steering Control Algorithm

Steering control of the autonomous vehicle began with the measurement of the tension cable angle. The angle was first converted into the vehicle lateral offset, which was used to determine the steering angle by a fuzzy logic controller (FLC).

Figure 7 presents the flowchart of the steering control algorithm. The guidance system is operated at a loop time of 10 ms. Due to the steering mechanism characteristics, the vehicle is steered when one steering clutch is disengaged, so that the actual steering angle is determined by the duration time of clutch disengagement. However, it requires at least 720 ms to complete a cycle of disengagement/re-engagement operation and additional time for maintaining the clutch disengagement. When the disengagement time is too short (less than 720 ms), activating the clutch may cause an adverse effect on the system performance, because it can not stop clutch operation in the interim and the guidance system can not update the current offset while the clutch is activated. A preliminary test showed that the vehicle moved in a zigzag when the required additional time was too small. Therefore, a deadband of 14 cm in the lateral offset was

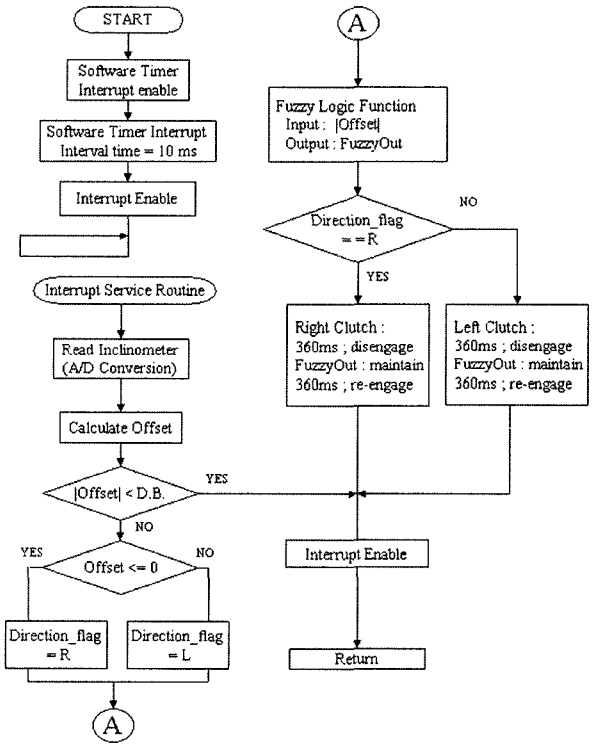

Fig. 7 Flowchart of steering control algorithm.

applied to the control algorithm and resulted in satisfactory performance. When the offset was smaller than the dead-band, the interrupt service routine would be terminated to maintain reading of the inclinometer data on the next interrupt signal. Otherwise, the control system determined which clutch should be activated based on the sign of the measured offset. Both power cylinders would not be activated concurrently to steer the vehicle.

The absolute value of the measured offset was quantified into linguistic variables to be used in the FLC. For an offset range from 0 to 120 cm, three linguistic variables of offset_small (OS), offset_medium (OM) and offset_large (OL) were defined using either triangular or trapezoid membership functions. The output from the FLC was a linguistic value of time duration for clutch disengagement. It also consisted of three singleton membership functions of time_small (TS), time_medium (TM) and time_large (TL) to represent a range of clutch disengagement time duration from 0 to 1.5 s, as shown in Fig. 8. If-Then type fuzzy control rules were developed based on vehicle steering experience. The fuzzy output was inferred using the Sugeno method of fuzzy inference and it was defuzzified by the weighted average method as in Eq. (3).

$$u_{wa}=\frac{\sum_{i=1}^{n}u_i\mu(u_i)}{\sum_{i=1}^{n}\mu(u_i)} \tag{3}$$

where $\mu(u_i)$ and u_i are the degree and singleton value of the i-th output membership function, respectively.

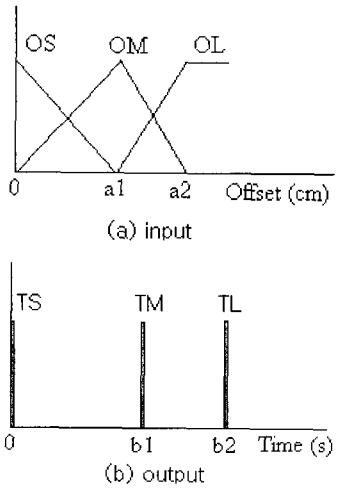

Fig. 8 Fuzzy membership functions.

Because the control system was synchronized with the interrupt signal generated every 10 ms, the final output was rounded to an integer of multiples of 10. When a steering action was initiated, the power cylinder was activated for clutch disengagement during 36 counts of the interrupt signal and maintained the state of disengagement for the duration of the output of the FLC. Then the power cylinder was retracted to re-engage the clutch during 36 counts of the interrupt signal. On completion of clutch re-engagement, a new interrupt signal was invoked to start a new A/D conversion. The control algorithm written in C was compiled by ic96 compiler and downloaded to the EPROM of the microprocessor.

E. Computer simulation

Through computer simulation the feasibility of the control system was investigated and the proper membership functions were determined. A mathematical model for the movement of the experimental vehicle was established using earth coordinates. As shown in Fig. 2, the initial position of the vehicle was provided in terms of the lateral offset and the heading angle from the location of the fifth wheel. The coordinates of the center of gravity (CG) could be obtained from the following :

$$\begin{Bmatrix}x(t)\\y(t)\end{Bmatrix}=\begin{bmatrix}\sin(\theta(t))\\\cos(\theta(t))\end{bmatrix}*CG2Fifth+\begin{bmatrix}\pm\ Offset\_Fifth\\0\end{bmatrix} \tag{4}$$

where *Offset_Fifth* is the initial lateral offset of the fifth wheel to the overhead guidance rail and the minus sign indicates that the vehicle is placed to the left of the overhead guidance rail. *CG2Fifth* is the distance from CG to the fifth wheel, and $\theta(t)$ is the current heading angle of the vehicle measured from an imaginary vertical line and has a minus value when the vehicle is making a left turn.

While the real autonomous guidance system began by measuring the offset by the inclinometer, the offset in the computer simulation was calculated by the geometry and the initial position of the vehicle as follows.

$$Offset=x(t)+CG2Clinometer*\sin(\theta(t)) \tag{5}$$

where *CG2Clinometer* is the distance from CG to the

inclinometer.

This value was input to the FLC to determine the time duration for the steering clutch to be maintained disengaged. The operation of the steering clutch can be characterized in 3 stages. Since the steering clutch used in the project was the jaw-type, the power to the driving sprocket was maintained until the teeth of the clutch were completely disengaged. This kept the vehicle traveling with the same heading angle. Therefore, the next position of CG for the first stage of clutch operation could be obtained as the following :

$$\begin{matrix}\begin{Bmatrix}x(t+1)\\y(t+1)\end{Bmatrix}=\begin{Bmatrix}x(t)\\y(t)\end{Bmatrix}+\begin{bmatrix}\sin(\theta(t))\\\cos(\theta(t))\end{bmatrix}*Vel*Intval\,Time\\\theta(t+1)=\theta(t)\end{matrix} \quad (6)$$

where *Vel* is the ground speed of the vehicle and *IntvalTime* is the control time, or interrupt time.

During the second stage of clutch operation the vehicle started steering. Since the driving power was transferred to only one track, the vehicle could pivot on the other track, in particular about the intersection of the extended line from CG toward the track and the centerline of the track. This made the vehicle turn around the center of the braked track, and the CG also turned around the same point. The track to be braked is determined by the current position of the vehicle. If the vehicle is positioned to the left of the guidance rail, it should turn right, which means that the right track will be the turning center. In the case of a right turn, the coordinates of the instant turning center on the right track could be obtained as follows.

$$\begin{Bmatrix}Cx(t)\\Cy(t)\end{Bmatrix}=\begin{Bmatrix}x(t)\\y(t)\end{Bmatrix}+\begin{bmatrix}\cos(\theta(t))\\-\sin(\theta(t))\end{bmatrix}*\frac{SSWidth}{2} \quad (7)$$

where SSWidth is the effective width of the centerlines of both tracks.

For a left turn, they should be

$$\begin{Bmatrix}Cx(t)\\Cy(t)\end{Bmatrix}=\begin{Bmatrix}x(t)\\y(t)\end{Bmatrix}+\begin{bmatrix}-\cos(\theta(t))\\\sin(\theta(t))\end{bmatrix}*\frac{SSWidth}{2} \quad (8)$$

When the vehicle turns about a pivot (*Cx(t), Cy(t)*), the turning angle, ϕ, during one control period can be calculated by

$$\phi=\frac{Vel*Intval\,Time}{SSWidth} \quad (9)$$

This angle is the heading angle change for the vehicle as it makes a turn for one control period.

When the vehicle makes a right turn, the next position of CG and the heading angle can be calculated based on the coordinates of the turning center, (*Cx(t), Cy(t)*) from Eq. (7) as follows :

$$\begin{matrix}\begin{Bmatrix}x(t+1)\\y(t+1)\end{Bmatrix}=\begin{bmatrix}\cos(\phi)&-\sin(\phi)\\\sin(\phi)&\cos(\phi)\end{bmatrix}\begin{Bmatrix}x(t)\\y(t)\end{Bmatrix}-\begin{bmatrix}\cos(\phi)-1&-\sin(\phi)\\\sin(\phi)&\cos(\phi)-1\end{bmatrix}\begin{Bmatrix}Cx(t)\\Cy(t)\end{Bmatrix}\\\theta(t+1)=\theta(t)+\phi\end{matrix} \quad (10)$$

In the same manner, referring to Eq. (8), the next position of CG in a left turn becomes

$$\begin{matrix}\begin{Bmatrix}x(t+1)\\y(t+1)\end{Bmatrix}=\begin{bmatrix}\cos(\phi)&\sin(\phi)\\-\sin(\phi)&\cos(\phi)\end{bmatrix}\begin{Bmatrix}x(t)\\y(t)\end{Bmatrix}-\begin{bmatrix}\cos(\phi)-1&\sin(\phi)\\-\sin(\phi)&\cos(\phi)-1\end{bmatrix}\begin{Bmatrix}Cx(t)\\Cy(t)\end{Bmatrix}\\\theta(t+1)=\theta(t)-\phi\end{matrix} \quad (11)$$

The turning process lasts for the duration of output of the FLC.

After completing the turn, as a third stage the clutch starts to be re-engaged. Similar to the first stage, the next position of CG of the vehicle is the same as in Eq. (6) and the vehicle moves straight forward for 360 ms with the previous heading angle.

On the other hand, the trajectory of the fifth wheel can be calculated by the geometry of the vehicle as follows.

$$\begin{Bmatrix}x\_fifth(t)\\y\_fifth(t)\end{Bmatrix}=\begin{Bmatrix}x(t)\\y(t)\end{Bmatrix}-\begin{bmatrix}\sin(\theta(t))\\\cos(\theta(t))\end{bmatrix}*CG2Fifth \quad (12)$$

The computer simulation was conducted based on the assumptions of a flat ground surface, no slippage, constant steering load, and zero deadband. In the simulation, setting up a deadband was not considered because it made the simulation result oscillate. For tuning the membership functions of the FLC as well as the performance evaluation, a series of computer simulations were executed on three different output fuzzy membership functions of B1 = {0, 0.8, 1.5} s, B2 = {0, 0.7, 1.3} s, and B3 = {0, 0.6, 1.1} s with the fixed input fuzzy variable of A = { 0, 70, 120} cm (as shown in Fig. 8) and ground speed levels of low (= 30 cm/s), middle (= 40 cm/s) and high (= 50 cm/s). The maximum deviations were obtained from the trajectories of CG of the vehicle on a

straight path only. The initial values of major simulation parameters are presented in Table 1.

F. System Evaluation

The performance of the autonomous guidance system was evaluated on a straight section and on a turning section over a flat surface as shown in Fig. 9. The first test was intended to investigate how accurately the guidance system could steer the vehicle on a straight path at three ground speeds with initial offset of 0 cm and initial heading angle of 0°. The true path of the vehicle was manually recorded every 20 cm from the trajectory of the fifth wheel attached to the rear end of the vehicle. Each deviation between the true path and the desired path (the projected line of the overhead guidance rail) was calculated .The system performance was represented by the root mean square (RMS) value of deviations as Cho and Ki (1999).

Secondly, a test was performed to investigate how quickly the vehicle was able to track the desired path, even when it started from a position with an initial offset and heading angle. The test conditions were the same as the initial conditions of the computer simulation in Table 1. For each initial condition, the data were acquired for three ground speeds. The third test was conducted on the turning section with three ground speeds. Total lengths of paths in which data were acquired were 7 m and 4 m for the straight path and the turning section, respectively.

Table 1 Major parameters in the computer simulation

Parameter	Initial value	Remark
Initial heading angle, (θ)	10°, 20°	at zero offset
Initial offset, *Offset_Fifth*	25 cm, 50 cm	at zero heading angle

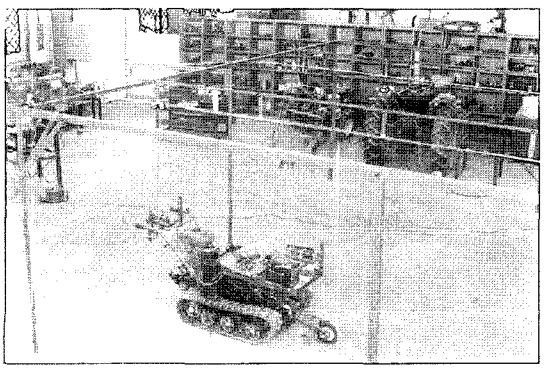

Fig. 9 Overall view of experimental setup.

3. RESULTS AND DISCUSSION

As the system performance index in the computer simulation, the maximum deviations at given initial conditions and output membership functions are presented in Table 2. It is needed that the maximum deviation should be as small as possible to avoid vehicle's colliding with trees. The simulation results showed that the maximum deviation increased as the offset and the heading angle increased for all tested output membership functions. Because the vehicle had to make an immediate turn with a large angle in the case of large offsets or heading angles. The output membership function B1 showed relatively low maximum deviations at low and middle ground speeds, however the maximum deviation greatly increased at high ground speed. In the case of membership function B2, the maximum deviation at high ground speed did not increase as much as in membership function B1. To be applicable in the range of all ground speeds, it is desirable to select the membership function which gives the smallest value among the greatest maximum deviations from each membership function. Therefore, B2 was selected as the output membership function for the guidance system.

The trajectory of the fifth wheel was calculated from the simulation results using Eq. (12) and was compared with the actual paths of the vehicle for the given initial conditions, as shown in Fig. 10. The results showed the same trends

Table 2 Magnitudes of maximum deviation on three fuzzy output membership functions

Offset	Heading angle	Ground speed	Fuzzy output membership function		
			B1	B2	B3
25 cm	0°	30 cm/s	8.09	8.26	10.82
		40 cm/s	7.60	8.61	13.44
		50 cm/s	13.67	10.66	11.59
50 cm	0°	30 cm/s	12.86	14.22	17.17
		40 cm/s	11.02	14.46	23.34
		50 cm/s	20.66	17.07	16.80
0 cm	10°	30 cm/s	6.46	7.24	8.16
		40 cm/s	7.57	9.45	10.69
		50 cm/s	8.43	6.02	14.21
0 cm	20°	30 cm/s	9.02	12.08	15.75
		40 cm/s	8.34	16.62	14.78
		50 cm/s	15.84	11.58	29.48

(Unit : cm)

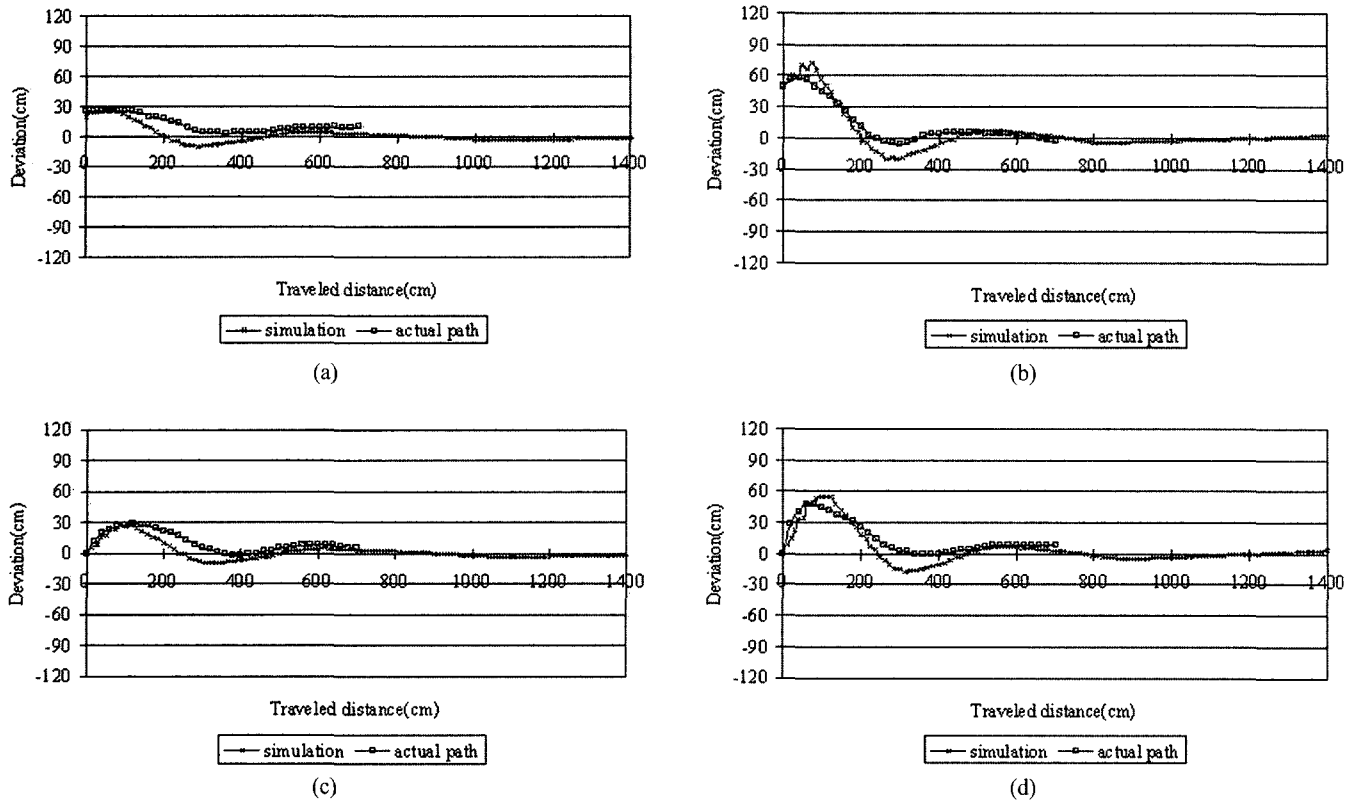

Fig. 10 Comparison of simulation results and actual path at low ground speed on various initial settings : (a) offset = 25 cm, (b) offset = 50 cm, (c) heading = 10°, and (d) heading = 20°.

between the actual and the simulation paths. However, the simulation path showed a greater steering angle than the actual path, and resulted in a zigzag along the trajectory of the vehicle. This indicated that the clutch did not work exactly for the specified length of time and the moving track did not make a clear turn around the pivot on the stationary track. It was also observed that the tension cable might not have adjusted the inclinometer accurately in the neighborhood of the centerline. These characteristics of the vehicle steering system and the slow steering actuator cause the vehicle to follow the desired path in a slower and smoother fashion than the simulation.

Fig. 10 Comparison of simulation results and actual path at low ground speed on various initial settings : (a) offset = 25 cm, (b) offset = 50 cm, (c) heading = 10°, and (d) heading = 20°.

Figures 11 ~ 13 show typical test results for the actual path of the vehicle on the straight path. Figure 11 depicts the case of the actual path starting with zero offset and zero heading angle for three ground speeds. Although steering

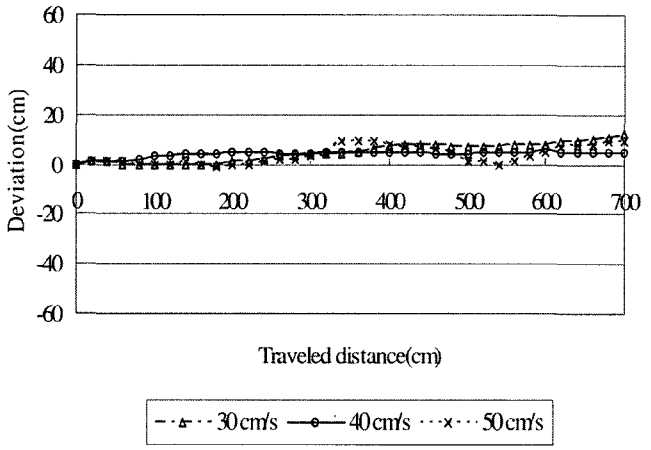

Fig. 11 Guidance system performance at three different ground speeds without any initial offset and heading angle.

action should not occur for these initial conditions, some steering action occurred because the ground surface condition caused the vehicle to steer unintentionally. In the case of low ground speed the deviation seemed to increase as the vehicle traveled because the vehicle was not steered until the deviation became greater than the deadband. It was observed that, at high ground speed, the vehicle tended to

zigzag along the path. The RMS values of each trial were 5.99, 4.35, 4.95 cm for low, middle, high ground speeds, respectively. The maximum deviations were less than 12 cm in all test trials. It was concluded that the guidance system could control the vehicle independently of ground speed.

Figure 12 shows the travel paths begun from locations with lateral offsets of 25 and 50 cm, respectively. All trials with both initial offsets showed that the vehicle was getting close to the desired path as it moved forward. It took 2 ~ 3 m for the vehicle to be steered within the range of deviation as with zero offset and zero heading angle. However, with a large initial offset as in Fig. 12-(b), the vehicle tended to overshoot the intended centerline before being steered back to the desired path.

Figure 13 shows the travel paths with initial heading angles of 10° and 20° toward the left from the location of the fifth wheel in the case of zero offset. For the small heading angle shown in Fig. 13-(a), the vehicle could move smoothly at low and middle ground speeds, but the phenomenon of oscillation was observed at high ground speed. Large initial heading angle at high ground speed caused an immediate skid-turn to the right, resulting in a left deviation measured at the rear end of the vehicle (Fig. 13-(b)). Similar to the previous results at different initial offsets, the steering of the vehicle could be controlled within the acceptable range of deviation after traveling the first 2 ~ 3 m to track the desired path.

Fig. 12 Guidance system performance at different lateral offsets with zero initial heading angle at different ground speeds.

Figure 14 shows the vehicle moving counterclockwise around the turning section of the guidance rail. Although the trajectories seem to be an outline of the desired path, this is, in fact, because they were measured at the rear of the

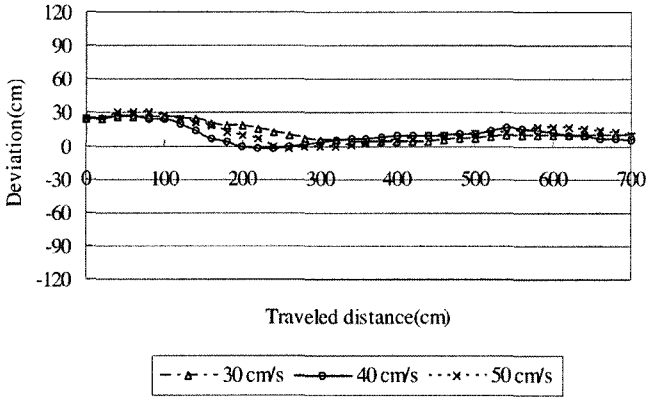

(a) 25 cm

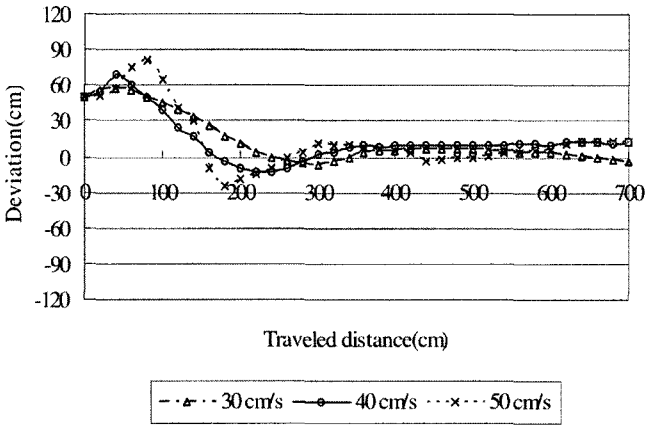

(b) 50 cm

Fig. 12 Guidance system performance at different lateral offsets with zero initial heading angle at different ground speeds.

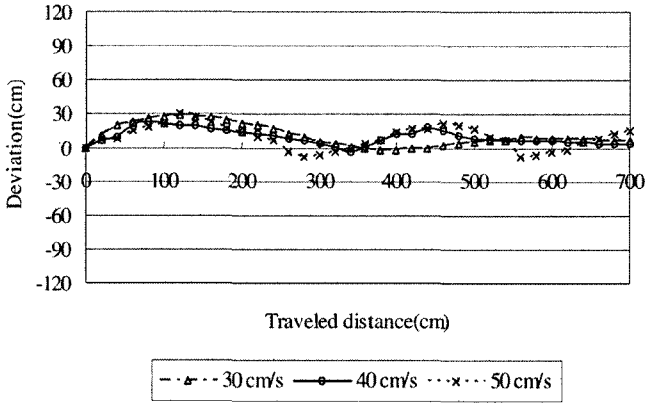

(a) 10°

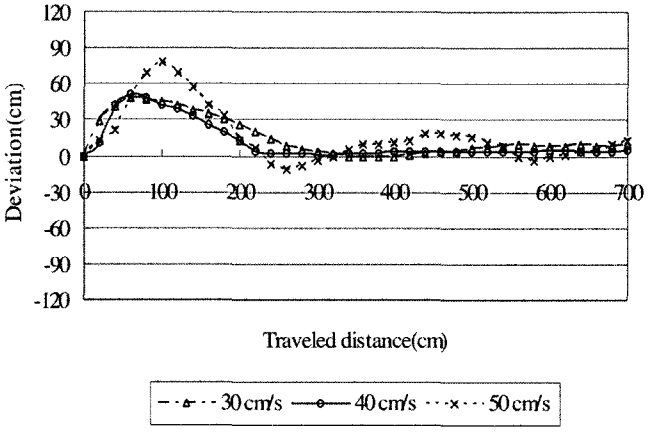

(b) 20°

Fig. 13 Guidance system performance for different heading angles with zero initial lateral offset at different ground speeds.

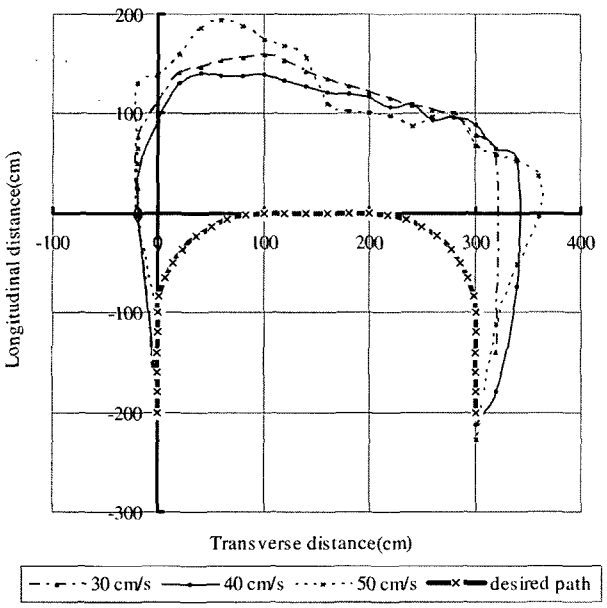

Fig. 14 Traveled path of vehicle at turning section.

vehicle. It was observed that the vehicle tended to move more outward as the ground speed increased. For all ground speeds, however, the guidance system could turn the vehicle reliably at the end of tree rows without an additional control algorithm. It was also proved that the trolley could move smoothly on a curved path of 1 m curvature.

4. CONCLUSIONS

Based on a mechanical sensory system and a microprocessor, an autonomous guidance system was developed for a small-scale track-tread orchard sprayer operated in very narrow and confined working environments such as in pear orchards or vineyards. The guidance system could steer the vehicle to follow overhead guidance rails with a RMS error of 5 cm within its normal travel speed range of 30 ~ 50 cm/s. The maximum deviation did not exceed 12 cm. Even if the vehicle started with an initial offset from the desired path or a deflected heading angle, the vehicle could follow the desired path within a short time. The major advantage of this guidance system is that it does not need an extra control algorithm to turn the vehicle at the end of tree rows. The trials showed that the vehicle could be reliably turned and set into the next row along the curved guidance rail with a curvature of 1 m, where the distance between tree rows was 3 m. However, the vehicle tended to be over-steered and zigzagged along the path as its ground speed increased. Since the effect of steering is determined by the steering clutch operation time, a shorter operating time is required to maneuver the vehicle smoothly as the vehicle speed increases. The over-steer at high ground speed is attributed to the actuation speed of the electrically-operated cylinder used in the guidance system. In addition, one lateral offset measured at the front of the vehicle can not provide an exact current heading angle of the vehicle, so that the zigzag motion appears. This phenomenon, amplified by the over-steering effect, makes the vehicle run zigzag at high ground speed. This guidance system turns out to be sufficiently practical and applicable to a slow-moving vehicle, due to the low cost microprocessor-based controller and the reliability of the mechanical sensory system.

For future work it is suggested that the lateral offset measurement system should be improved to provide the current heading angle of the vehicle as well as the accurate lateral offset. This can be accomplished either by measurement of lateral offsets at two points, the front and rear ends of the vehicle, or by a triangular arrangement of connecting cables using one point on the overhead guidance rail and two points on the vehicle. Replacements for jaw-type steering clutches in such vehicles and high speed actuators are recommended.

REFERENCES

1. Cho, S. I. and J. H. Lee. 2000. Autonomous speed sprayer using differential positioning system, genetic algorithm and fuzzy control. J. Agric. Engng Res. 76(2):111-119.
2. Cho, S. I. and N. H. Ki. 1999. Autonomous speed sprayer guidance using machine vision and fuzzy logic. Transactions of the ASAE 42(4):1137-1143.
3. Jang, I. J., T. H. Kim and M. D. Cho. 1995. Development of unmanned speed sprayer- (Part I): Remote control and induction cable system. Journal of the Korean Society of Agricultural Machinery 20(3):209-216. (in Korean)
4. Kim, T. H., I. J. Jang and C. T. Kang. 1999. Development of autonomous sprayer for greenhouse using guide pipe(I) - Self-propelled system - Journal of the Korean Society of Agricultural Machinery 24(3): 209-216. (in Korean)
5. Shin, B. S., S. H. Kim and Y. M. Koo, 2001. Autonomous

guidance using ultrasonic sensors for small orchard sprayer. J. Agric. & Bio. Eng. 2:33-43.
6. Siemens, M. C. and W. E. Coates. 2000. Control system for the mobile truss of a cable-drawing farming system. Applied Engineering in Agriculture 16(3):211-216.
7. Torri, T. 2000. Research in autonomous agriculture vehicles in Japan. Comput. Electron. Agric. 25:133-153.